Scientific Research Publishing

Advances in Nanoparticles, 2025, 14(3), 91-99
https://www.scirp.org/journal/anp
ISSN Online: 2169-0529
ISSN Print: 2169-0510

Morphology-Tailored, Mixed-Dimensional $CsPbBr_3$ Nanostructures for Efficient Light Emission

Nidhi Kumari[1], Mamraj Singh[1], Narendra Singh Leel[2]

[1]Department of Physics, University of Rajasthan, Jaipur, India
[2]Department of Pure and Applied Physics, University of Kota, Kota, India
Email: nidhi.meena.2986@gmail.com

How to cite this paper: Kumari, N., Singh, M. and Leel, N.S. (2025) Morphology-Tailored, Mixed-Dimensional $CsPbBr_3$ Nanostructures for Efficient Light Emission. *Advances in Nanoparticles*, **14**, 91-99.
https://doi.org/10.4236/anp.2025.143006

Received: July 18, 2025
Accepted: August 16, 2025
Published: August 19, 2025

Abstract

$CsPbBr_3$ nanowires (NWs) and nanocrystals (NCs) were synthesized via a solution-phase method and systematically characterized to evaluate their structural and optical properties. Field emission scanning electron microscopy (FESEM) and high-resolution transmission electron microscopy (HRTEM) revealed mixed-dimensional nanostructures, including NWs up to ~15 μm in length and NCs with different morphologies. X-ray diffraction (XRD) confirmed the orthorhombic phase with sharp reflections and characteristic peak splitting, indicating high phase purity. Lattice fringes with ~0.30 nm spacing were observed in HRTEM, and selected area electron diffraction (SAED) confirmed the single-crystalline nature of the NCs. UV-Vis absorption showed a primary excitonic peak at ~520 nm, complemented by a sharp photoluminescence (PL) peak at 526 nm with a FWHM of ~23 nm. The small Stokes shift indicates minimal trap-related recombination, which is useful for high-performance optoelectronic applications.

Keywords

$CsPbBr_3$, Nanowires, Nanostructures, Photoluminescence, Stokes Shift, Perovskite, Optoelectronic Materials

1. Introduction

Metal halide perovskites have attracted considerable interest for optoelectronic applications [1]-[3]. These materials generally adopt the AMX_3 structure, where A is a monovalent cation (e.g., Cs^+), M is a divalent metal ion (e.g., Pb^{2+}), and X represents a halide ion (e.g., Cl^-, Br^-) [4].

Cesium lead bromide ($CsPbBr_3$) has emerged as a highly attractive perovskite for optoelectronic devices due to its direct bandgap, strong PL, and long carrier diffusion lengths [3]-[5]. Its fully inorganic composition offers improved thermal and environmental stability over hybrid perovskites, making it well-suited for applications such as LEDs, photodetectors, and nanophotonic components [3] [4] [6]-[13].

Controlled synthesis of $CsPbX_3$ with tunable shapes has been widely explored through colloidal methods [4]-[6] [14]-[17]. Time-dependent growth strategies have enabled the transition from nanocubes to NWs and nanosheets, with intermediate stages yielding mixed morphologies [14]. Room-temperature reprecipitation techniques have also enabled the formation of green-emitting nanoplatelets and nanosheets with controlled lateral dimensions [6] [15] [16] [18]. Additionally, temperature has been identified as a critical factor influencing anisotropic growth [18]. These studies underscore the critical role of synthesis conditions in controlling the dimensionality and optical response of $CsPbBr_3$ nanostructures.

In this work, we report a solution-phase synthesis of $CsPbBr_3$ NWs and NCs, yielding mixed-dimensional structures and morphology. The synthesized nanostructures exhibit a highly crystalline orthorhombic phase, strong green emission with a narrow PL linewidth, and a ~6 nm Stokes shift, demonstrating their potential for high-efficiency optoelectronic applications.

2. Experimental

2.1. Materials and Methods

Cesium carbonate (Cs_2CO_3, 99.9%), 1-octadecene (ODE, 90%, technical grade), oleic acid (OA, 90%, technical grade), oleylamine (OAm, 70%), lead (II) bromide ($PbBr_2$, 99.999%), and anhydrous toluene (99%) were purchased from Sigma-Aldrich. Tert-butanol (t-BuOH, 90%) was obtained from Loba Chemie. All chemicals were used as received without further purification.

2.2. Synthesis of $CsPbBr_3$ Nanostructures

$CsPbBr_3$ nanocrystals with green luminescence were synthesized following a hot-injection method reported in previous studies [17] [18]. The precursor amounts, ratios, and purification procedures are described in detail in the cited references (see **Figure 1** for details). In short, cesium oleate was prepared by dissolving Cs_2CO_3 in ODE and OA at 120˚C under vacuum. Separately, $PbBr_2$, OAm, OA, and ODE were heated under similar conditions; then, 0.4 mL of hot Cs-oleate was injected at 140˚C under N_2, quenched after 15 seconds, and the product was centrifuged, washed (with Tert-butanol) and redispersed in toluene.

2.3. Characterization Techniques

The surface morphology and crystalline structure were examined using FESEM (JEOL JSM-7610F Plus) and HRTEM (Tecnai G2 20 S-TWIN (FEI, 200 kV)). The crystal structure was determined using a PANalytical X'Pert Pro diffractometer

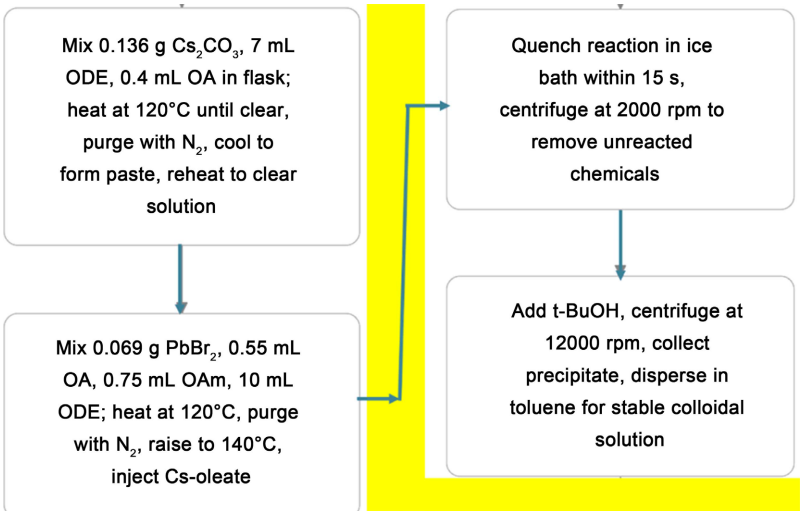

Figure 1. Four-step synthesis of perovskite nanostructures: from cesium oleate preparation to stable colloidal solution.

with Cu-Kα radiation (λ = 1.5406 Å). Optical absorption spectra were recorded using an Agilent Cary 5000 UV-Vis-NIR spectrophotometer. PL measurements were carried out using a custom-built setup equipped with a 400 nm diode laser.

3. Results and Discussion

3.1. Surface Morphology Analysis

FESEM was employed to investigate the surface morphology of the synthesized $CsPbBr_3$ nanostructures presented in **Figure 2**. **Figure 2(a)** presents a FESEM image showing a mixture of NWs and NCs, including micrometer-sized cubes and elongated structures. **Figure 2(b)** provides a high-resolution image of the NWs, NCs, and micron-sized rods and cubic crystals. **Figure 2(c)** displays NWs extending up to 15 μm in length with diameters of approximately 200 nm. **Figure 2(d)** shows a closer view of an individual NW, highlighting its uniform morphology and high aspect ratio. These observations confirm the successful synthesis of mixed-dimensional $CsPbBr_3$ nanostructures with well-defined morphology. FESEM images reveal a mixture of NWs and NCs, with cubic particles and elongated nanowires observed across the sample (**Figures 2(a)-(d)**). NWs with diameters < 200 nm and L ~15 μm were confirmed by high-magnification imaging.

The formation of mixed-dimensional $CsPbBr_3$ nanostructures, such as nanowires (NWs) and nanocubes (NCs), arises from the interplay between precursor availability, ligand coordination, and reaction kinetics during hot-injection synthesis [7] [18]-[20]. A moderate volume of octadecene (~10 mL) maintains optimal monomer concentration, enabling controlled nucleation [7] [19]. Oleylamine (OAm) and oleic acid (OA) act as dynamic ligands, selectively passivating crystal facets and directing anisotropic growth [19]. At a reaction temperature of 140˚C, anisotropic growth is favored due to sufficient thermal energy overcoming nucleation barriers, consistent with the kinetic model described by Zhang *et al.* (2020)

[7]. Rapid quenching of the reaction in an ice bath effectively arrests further growth, preserving the elongated morphology of NWs [7]. This approach yields a heterogeneous mixture of NWs (~15 μm) and NCs, in agreement with earlier reports [7] [19].

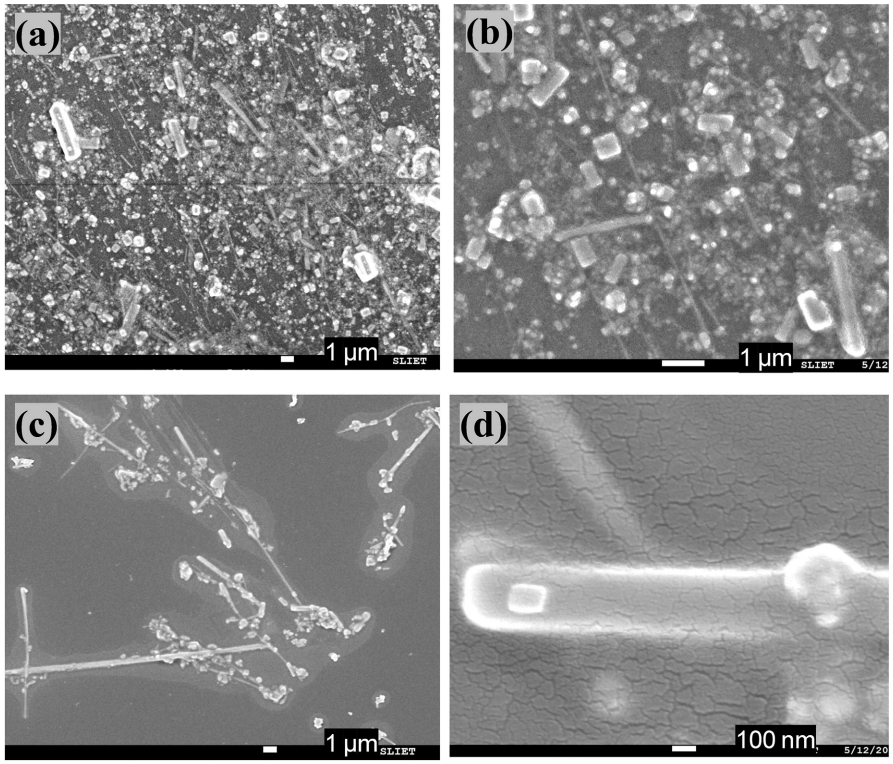

Figure 2. (a) Low-magnification FESEM image of $CsPbBr_3$ NWs and NCs, displaying a mixture of morphologies including microcrystals and nanorod structures; (b) higher magnification image revealing the coexistence of NWs, NCs, and micron-sized rods; (c) NWs with lengths up to ~15 μm and diameters around 200 nm; (d) close-view of a single NW.

3.2. Microstructural and Crystallographic Analysis

HRTEM was employed to further investigate the structural and crystallographic features of the $CsPbBr_3$ NWs and NCs. **Figure 3(a)** shows a bundle of NWs with diameters below 200 nm and lengths of approximately 1 μm. **Figure 3(b)** presents the surface morphology of an individual NW. The high-resolution image in **Figure 3(c)** displays lattice fringes of average interplanar d-spacing ~0.30 nm of the $CsPbBr_3$ NWs. This value is consistent with the d-spacing corresponding to the XRD peak at $2\theta \approx 29.02^{\circ}$ (see **Figure 4**). The SAED pattern in **Figure 3(d)** displays discrete diffraction spots, confirming the single-crystalline nature of the NWs. SAED patterns (**Figure 3(d)**).

3.3. Crystal Structure (XRD) Analysis

The XRD pattern (**Figure 4**) exhibits prominent diffraction peaks at 2θ ~14.64˚, 14.79˚, 29.97˚, 30.28˚, 41.74˚, and 62.84˚ and confirms that the synthesized $CsPbBr_3$ material exhibits a highly crystalline structure.

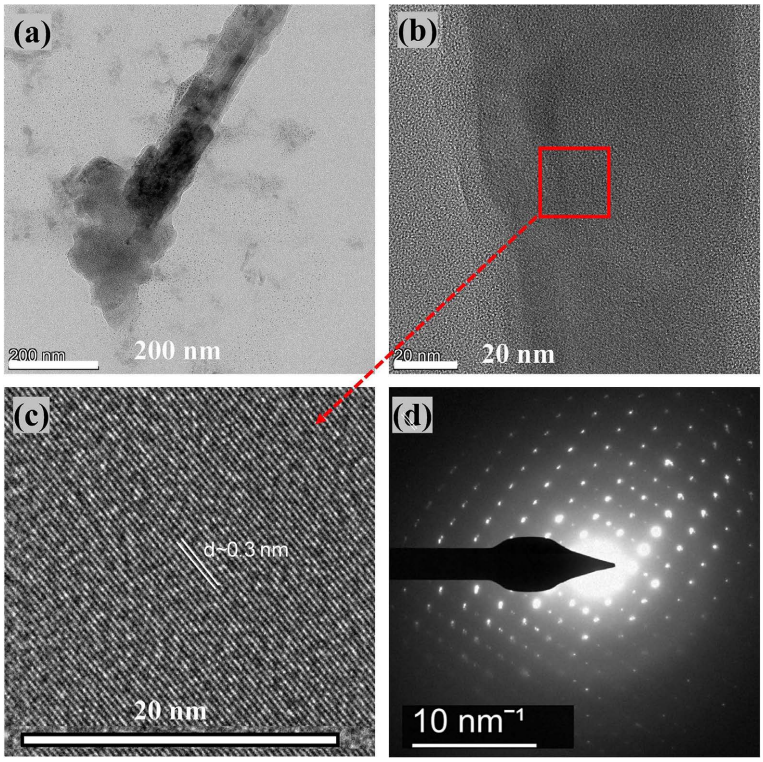

Figure 3. (a) HRTEM image showing a bundle of $CsPbBr_3$ NWs with diameters < 200 nm and lengths ~1 μm; (b) surface morphology of a single NW; (c) high-resolution image of lattice fringes; (d) SAED pattern displaying distinct diffraction spots, confirming the single-crystalline nature of the NW.

These peaks are consistent with the reference orthorhombic phase from ICSD #97851 [12] [21]. The observed peak splitting at ~14.6˚ and ~30.0˚ is characteristic of the orthorhombic phase and confirms deviation from the higher-symmetry cubic structure. The sharpness and intensity of these peaks indicate good crystallinity, with estimated crystallite sizes in the range of 50 - 100 nm based on the Scherrer equation [22].

It is important to note that the Scherrer method reflects the size of coherently diffracting crystalline domains, which can be considerably smaller than the overall physical dimensions of the nanostructures observed via FESEM, such as the nanowires up to 15 μm in length [23].

The identification of the orthorhombic phase holds considerable importance for optoelectronic applications. Unlike the more symmetric cubic phase, the orthorhombic structure offers greater thermodynamic stability at ambient conditions and is often associated with a marginally larger band gap and stronger exciton binding. These characteristics can enhance the photostability and improve charge carrier behavior in device performance [24]-[26].

3.4. Optical Properties

Figure 5 shows the UV-Vis absorption and PL spectra for the NWs and NCs. The inset displays the sample under ambient light, appearing yellow, and under

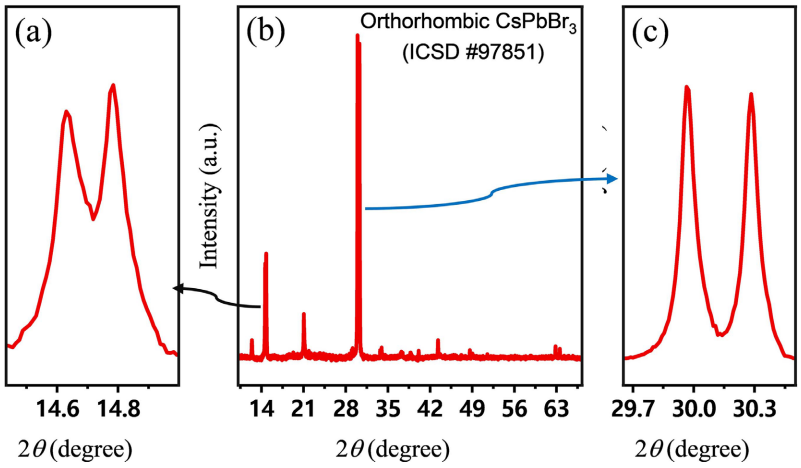

Figure 4. XRD pattern of (b) $CsPbBr_3$ showing sharp peaks consistent with the orthorhombic phase (ICSD #97851). Side figures (a) and (c) highlight the characteristic peak splitting near $2\theta \sim 14.6^\circ$ and $\sim 30.0^\circ$, respectively.

400 nm laser excitation, exhibiting bright green luminescence, indicative of efficient radiative recombination [6]. The UV-Vis spectrum reveals two absorption features with onsets near 396 nm and 520 nm, consistent with previously reported transitions in anisotropic and confined $CsPbBr_3$ nanostructures [18]. PL measurements reveal a strong peak at ~526 nm with a FWHM of ~23 nm. The ~6 nm Stokes shift between the absorption edge and emission peak indicates efficient excitonic emission and trap-assisted recombination and confirms the presence, typical of high-quality perovskite nanostructures [27] [28]. Photographs under 400 nm excitation show strong green luminescence, confirming efficient radiative recombination, in line with the observed optical data. These results demonstrate that the $CsPbBr_3$ nanostructures possess excellent light-emitting properties.

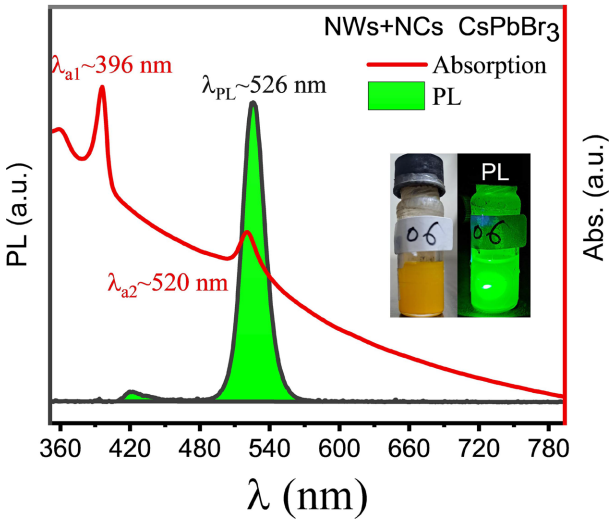

Figure 5. UV-Vis absorption and PL spectra of $CsPbBr_3$ NWs and NCs and an image of the sample (ambient light (yellow) and under 400 nm excitation (green luminescence)). The PL peak (526 nm, FWHM ~23 nm) indicates strong emission and high optical quality.

4. Conclusion

Morphology-controlled $CsPbBr_3$ NWs and NCs were synthesized and characterized, exhibiting phase-pure orthorhombic structure and excellent luminescent properties. HRTEM and XRD analyses confirmed high crystallinity and structural integrity, while optical characterization revealed strong green emission with minimal Stokes shift. These findings demonstrate the potential of $CsPbBr_3$ nanostructures for optoelectronic devices.

Acknowledgements

The authors gratefully acknowledge the Head, Department of Physics, University of Rajasthan, for providing access to the UV-Vis spectroscopy facility.

Conflicts of Interest

The authors declare no conflicts of interest regarding the publication of this paper.

References

[1] Stranks, S.D., Eperon, G.E., Grancini, G., Menelaou, C., Alcocer, M.J.P., Leijtens, T., *et al.* (2013) Electron-Hole Diffusion Lengths Exceeding 1 Micrometer in an Organometal Trihalide Perovskite Absorber. *Science*, **342**, 341-344. https://doi.org/10.1126/science.1243982

[2] Shang, Y., Liao, Y., Wei, Q., Wang, Z., Xiang, B., Ke, Y., *et al.* (2019) Highly Stable Hybrid Perovskite Light-Emitting Diodes Based on Dion-Jacobson Structure. *Science Advances*, **5**, 1-9. https://doi.org/10.1126/sciadv.aaw8072

[3] Dey, A., Ye, J., De, A., Debroye, E., Ha, S.K., Bladt, E., *et al.* (2021) State of the Art and Prospects for Halide Perovskite Nanocrystals. *ACS Nano*, **15**, 10775-10981. https://doi.org/10.1021/acsnano.0c08903

[4] Otero-Martínez, C., Ye, J., Sung, J., Pastoriza-Santos, I., Pérez-Juste, J., Xia, Z., *et al.* (2022) Colloidal Metal-Halide Perovskite Nanoplatelets: Thickness-Controlled Synthesis, Properties, and Application in Light-Emitting Diodes. *Advanced Materials*, **34**, Article 2107105. https://doi.org/10.1002/adma.202107105

[5] Rashid, M.U., Tahir, Z., Sheeraz, M., Ullah, F., Park, Y.C., Maqbool, F., *et al.* (2024) Controlled Morphological Growth and Photonic Lasing in Cesium Lead Bromide Microcrystals. *Nanomaterials*, **14**, Article 1248. https://doi.org/10.3390/nano14151248

[6] Abiedh, K., Salerno, M., Hassen, F. and Zaaboub, Z. (2024) Single $CsPbBr_3$ Perovskite Microcrystals: From Microcubes to Microrods with Improved Crystallinity and Green Emission. *Materials*, **17**, Article 4043. https://doi.org/10.3390/ma17164043

[7] Zhang, L., Zhang, Y., He, W., Peng, H. and Dai, Q. (2020) $CsPbBr_3$ Perovskite Nanowires and Their Optical Properties. *Optical Materials*, **109**, Article 110399. https://doi.org/10.1016/j.optmat.2020.110399

[8] Su, L. (2024) Room Temperature Growth of $CsPbBr_3$ Single Crystal for Asymmetric MSM Structure Photodetector. *Journal of Materials Science & Technology*, **187**, 113-122. https://doi.org/10.1016/j.jmst.2024.01.003

[9] Hua, F., Du, X., Huang, Z., Gu, Y., Wen, J., Liu, F., *et al.* (2024) Self-Powered Photodetector Based on a $CsPbBr_3$/n-Si Schottky Junction. *Journal of the Optical Society of America B*, **41**, 55-61. https://doi.org/10.1364/josab.503296

[10] Han, Q., Wang, J., Tian, S., Hu, S., Wu, X., Bai, R., *et al.* (2024) Inorganic Perovskite-Based Active Multifunctional Integrated Photonic Devices. *Nature Communications*, **15**, Article No. 1536. https://doi.org/10.1038/s41467-024-45565-9

[11] Almeida da Silva, T.C., Sánchez, R.S., Alberola-Borràs, J., Vidal, R., Mora-Seró, I. and Julián-López, B. (2025) Advancing Scalability and Sustainability of Perovskite Light-Emitting Diodes through the Microwave Synthesis of Nanocrystals. *Energy & Environmental Materials*, **8**, e12810. https://doi.org/10.1002/eem2.12810

[12] Sujith, P., Pratheek, M., Parne, S.R. and Predeep, P. (2023) Growth and Characterization of High-Quality Orthorhombic Phase $CsPbBr_3$ Perovskite Single Crystals for Optoelectronic Applications. *Journal of Electronic Materials*, **52**, 718-729.

[13] Zhang, X., Bai, R., Fu, Y., Hao, Y., Peng, X., Wang, J., *et al.* (2024) High Energy Resolution $CsPbBr_3$ Alpha Particle Detector with a Full-Customized Readout Application Specific Integrated Circuit. *Nature Communications*, **15**, Article No. 6333. https://doi.org/10.1038/s41467-024-50746-7

[14] Zhang, D., Eaton, S.W., Yu, Y., Dou, L. and Yang, P. (2015) Solution-Phase Synthesis of Cesium Lead Halide Perovskite Nanowires. *Journal of the American Chemical Society*, **137**, 9230-9233. https://doi.org/10.1021/jacs.5b05404

[15] Sun, S., Yuan, D., Xu, Y., Wang, A. and Deng, Z. (2016) Ligand-Mediated Synthesis of Shape-Controlled Cesium Lead Halide Perovskite Nanocrystals via Reprecipitation Process at Room Temperature. *ACS Nano*, **10**, 3648-3657. https://doi.org/10.1021/acsnano.5b08193

[16] Akkerman, Q.A., Motti, S.G., Srimath Kandada, A.R., Mosconi, E., D'Innocenzo, V., Bertoni, G., *et al.* (2016) Solution Synthesis Approach to Colloidal Cesium Lead Halide Perovskite Nanoplatelets with Monolayer-Level Thickness Control. *Journal of the American Chemical Society*, **138**, 1010-1016. https://doi.org/10.1021/jacs.5b12124

[17] Kushavah, D., Mushtaq, A. and Pal, S.K. (2023) Ultrafast and Nonlinear Optical Properties of Two-Dimensional Mo-Doped Dual Phase Inorganic Lead Halide Perovskite. *The Journal of Physical Chemistry C*, **127**, 20014-20025. https://doi.org/10.1021/acs.jpcc.3c02307

[18] Shamsi, J., Dang, Z., Bianchini, P., Canale, C., Di Stasio, F., Brescia, R., *et al.* (2016) Colloidal Synthesis of Quantum Confined Single Crystal $CsPbBr_3$ Nanosheets with Lateral Size Control up to the Micrometer Range. *Journal of the American Chemical Society*, **138**, 7240-7243. https://doi.org/10.1021/jacs.6b03166

[19] Zhou, J., Zhao, X., Jiang, Y., Zhou, Q., He, Y., Rui, J., *et al.* (2025) Optimizing $CsPbBr_3$ Nanowires for High-Performance Optoelectronics: Focusing on Blue Shift and Superfast Kinetics through Amine-Rich Synthesis. *Journal of Materials Chemistry C*, **13**, 7664-7670. https://doi.org/10.1039/d4tc05078a

[20] Haydous, F., Gardner, J.M. and Cappel, U.B. (2021) The Impact of Ligands on the Synthesis and Application of Metal Halide Perovskite Nanocrystals. *Journal of Materials Chemistry A*, **9**, 23419-23443. https://doi.org/10.1039/d1ta05242j

[21] Kostopoulou, A., Sygletou, M., Brintakis, K., Lappas, A. and Stratakis, E. (2017) Low-Temperature Benchtop-Synthesis of All-Inorganic Perovskite Nanowires. *Nanoscale*, **9**, 18202-18207. https://doi.org/10.1039/c7nr06404g

[22] Holzwarth, U. and Gibson, N. (2011) The Scherrer Equation versus the Debye-Scherrer Equation. *Nature Nanotechnology*, **6**, 534-534. https://doi.org/10.1038/nnano.2011.145

[23] Hassanzadeh-Tabrizi, S.A. (2023) Precise Calculation of Crystallite Size of Nanomaterials: A Review. *Journal of Alloys and Compounds*, **968**, Article 171914.

https://doi.org/10.1016/j.jallcom.2023.171914

[24] Wang, W., Wu, Y., Wang, D. and Zhang, T. (2019) Effective Control of the Growth and Photoluminescence Properties of $CsPbBr_3/Cs_4PbBr_6$ Nanocomposites by Solvent Engineering. *ACS Omega*, **4**, 19641-19646. https://doi.org/10.1021/acsomega.9b02248

[25] Protesescu, L., Yakunin, S., Bodnarchuk, M.I., Krieg, F., Caputo, R., Hendon, C.H., *et al.* (2015) Nanocrystals of Cesium Lead Halide Perovskites ($CsPbX_3$, X=Cl, Br, and I): Novel Optoelectronic Materials Showing Bright Emission with Wide Color Gamut. *Nano Letters*, **15**, 3692-3696. https://doi.org/10.1021/nl5048779

[26] López, C.A., Abia, C., Alvarez-Galván, M.C., Hong, B., Martínez-Huerta, M.V., Serrano-Sánchez, F., *et al.* (2020) Crystal Structure Features of $CsPbBr_3$ Perovskite Prepared by Mechanochemical Synthesis. *ACS Omega*, **5**, 5931-5938. https://doi.org/10.1021/acsomega.9b04248

[27] Xing, J., Zhao, Y., Askerka, M., Quan, L.N., Gong, X., Zhao, W., *et al.* (2018) Color-stable Highly Luminescent Sky-Blue Perovskite Light-Emitting Diodes. *Nature Communications*, **9**, Article No. 3541. https://doi.org/10.1038/s41467-018-05909-8

[28] da Silva, T.C.A., Fernández-Saiz, C., Sánchez, R.S., Gualdrón-Reyes, A.F., Mora-Seró, I. and Julián-López, B. (2025) A Soft-Chemistry Route to Prepare Halide Perovskite Nanocrystals with Tunable Emission and High Optical Performance. *Journal of Sol-Gel Science and Technology*, **114**, 131-138. https://doi.org/10.1007/s10971-023-06171-1